Composite Structures 106 (2013) 288–295

Contents lists available at SciVerse ScienceDirect

Composite Structures

journal homepage: www.elsevier.com/locate/compstruct

A general exact solution for heat conduction in multilayer spherical composite laminates

M. Norouzi *, A. Amiri Delouei, M. Seilsepour

Mechanical Engineering Department, Shahrood University of Technology, Shahrood, Iran

ARTICLE INFO

Article history:
Available online 25 June 2013

Keywords:
Analytical solution
Spherical composite laminate
Heat conduction
Fourier–Legendre series
Thomas algorithm

ABSTRACT

In this study, an exact analytical solution for steady conductive heat transfer in multilayer spherical fiber reinforced composite laminates is presented as the first time. Here, the orthotropic temperature distribution of laminate is obtained under the general linear boundary conditions that are suitable for various conditions including combinations of conduction, convection, and radiation both inside and outside of the sphere. The temperature and heat flux continuity is applied between the laminas. In order to obtain the exact solution, the separation of variables method is used and the set of equations related to the coefficient of Fourier–Legendre series of temperature distribution is solved using the recursive Thomas algorithm. The capability of the present solution is examined by applying it on two industrial applications for different fiber arrangements of multilayer spherical laminates.

1. Introduction

The fiber reinforced multilayer composite materials have interested significantly in modern engineering. This fact is due to vast advantages of these materials like high strength-to-density ratio, stiffness-to-density ratio, high corrosion resistance and plasticity as compared with most materials. Most of these unique advantages are because of two properties of these materials i.e. (1) combining different physical, mechanical and thermal properties of various materials; and (2) ability to change the fibers' orientations of every layer to meet the design requirements. Furthermore, increasing the more effective manufacturing technologies of composite materials accumulated over the years caused decreasing the cost of these kind of materials. Today, reinforced composites have been used enormously in aerospace and marine industries, pressure vessels, fluid reservoirs, pipes and so on. Although, the knowledge of composite materials has a reasonable progressive with the development of their applications, for example mechanical analysis [1–7], but thermal analysis is an exception. Heat transfer in composite laminates is vital for analyzing of thermal stress [8], thermal shock [9], controlling directional heat transfer through laminates and fiber placement in production processes [10,11].

The problem of heat conduction in multilayer structures can be subdivided based on the coordinates of solutions as: heat conduction in Cartesian coordinate [12–21], cylindrical coordinate in $r-z$ [22–27], and $r-\varphi$ [28,29] directions; and heat transfer in spherical shapes [30,31].

Blanc and Touratier [12] present a new simple refined computational model to analyze heat conduction in composite laminates. This model was based on an equivalent single layer approach allows to satisfy the continuity of temperatures and the heat flux between the layers, as well as the boundary conditions.

Separation of variables technique was used by Miller and Weaver [13] to predict the temperature distribution through a multi-layered system subject to complex boundary conditions. The system is subjected to both convection and radiation boundary conditions and results agree well with numerical results under the same boundary conditions.

Ma et al. [14,15] developed a closed-form solution for heat conduction in an anisotropic single layer [14] and multi-layered [15] media. A linear coordinate transformation is used to simplify the problem into an equivalent isotropic one.

Salt [16,17] investigated the response of a 2-D multi-layer composite slab, to a sudden temperature change. The solution is analytically examined in two- and three-layer composite slabs. Monte [18–21] developed several analytical solutions for heat conduction in 2-D composites.

Kayhani et al. [22–24] presented an exact analytical solution for axisymmetric steady heat conduction in cylindrical multi-layer composite laminates. The unsteady solution of this problem has been presented by Amiri Delouei et al. [25]. In these studies, a new Fourier transformation has been developed for steady and unsteady cases. Furthermore the Meromorphic function method was utilized to find the transient temperature distribution in laminate. Also, some studies have been investigated the conductive heat

* Corresponding author. Tel.: +98 9123726933; fax: +98 2733300258.
E-mail addresses: mnorouzi@shahroodut.ac.ir (M. Norouzi), a.a.delouei@gmail.com (A. Amiri Delouei), ms.mohsenseilsepour@gmail.com (M. Seilsepour).

0263-8223/$ - see front matter © 2013 Elsevier Ltd. All rights reserved.
http://dx.doi.org/10.1016/j.compstruct.2013.06.005

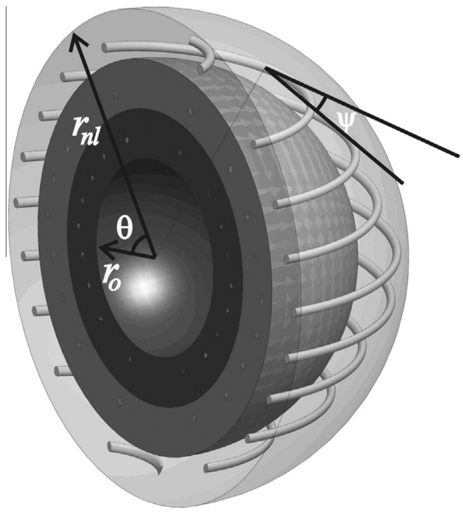

Fig. 1. Direction of fibers in a spherical laminate.

transfer in cylinders made from a functional graded material and composite laminates [26,27].

The asymmetric steady and transient heat conduction in cylindrical composite laminates have been studied by Kayhani et al. [28] and Norouzi et al. [29], respectively. Separation of variables method and Laplace Transformation was used to solve the partial differential equations. The solution they obtained is only valid for long pipes and vessels.

Only few studies have considered heat conduction of spherical multi-layered materials. Jain et al. [30,31] proposed an analytical series solution for heat conduction in $r-\theta$ spherical coordinates. Although this solution is valid for different kind of boundary conditions but materials in each layer have been considered in isotropic type. This solution is valid only for multi-layer spheres and cannot apply for multi-layer rein-forced composites spheres.

In this study, an exact analytical solution for steady state heat conduction in spherical composite laminates is presented. Laminates are in spherical shape (see Fig. 1) and composed from matrix and fiber materials. Heat conduction is considered in $r-\theta$ directions where r and θ represent radius and cone angle, respectively. Fibers are winded in circumferential direction (Fig. 1). The boundary conditions are the general linear boundary conditions which can simplified to all mechanisms of heat transfer both inside and outside of laminate. Governing equation of orthotropic heat conduction in each layer has been achieved and solved based on the separation of variables method. Using the separation of variables method, the solution can be reduced to the expansion of an arbitrary function into a series of Legendre polynomials. Considering the thermal boundary conditions inside and outside the cylinder, and applying the continuity of the temperature and the heat flux between the layers, the Fourier–Legendre coefficients are obtained. The Thomas algorithm is used to obtain the solution of the set of equations related to the temperature distribution coefficients. To our knowledge, this general analytical solution for spherical reinforced composite is the first one in this field. The ability of current solution is examined via two industrial examples consist of a composite vessel and a composite shell. The effect of composite thermal design parameters, i.e. fiber's direction and composite material of each layer, are investigated in details.

2. Conduction in spherical composites

In this section, the equations of conductive heat transfer in spherical composite materials are presented. The Fourier equation of orthotropic material in spherical coordinate system is as follows [32]:

$$\begin{pmatrix} q_r \\ q_\theta \\ q_\phi \end{pmatrix} = -\begin{bmatrix} k_{11} & k_{12} & k_{13} \\ k_{21} & k_{22} & k_{23} \\ k_{31} & k_{32} & k_{33} \end{bmatrix} \begin{pmatrix} \frac{\partial T}{\partial r} \\ \frac{1}{r}\frac{\partial T}{\partial \theta} \\ \frac{1}{r\sin\theta}\frac{\partial T}{\partial \phi} \end{pmatrix} \tag{1}$$

where k is the conductive heat transfer coefficient, T and q are temperature and heat flux, respectively. According to thermodynamic reciprocity, the tensor of conductive heat coefficients should be symmetric:

$$k_{ij} = k_{ji} \tag{2a}$$

On the other hand, the second law of thermodynamics caused that the diametric elements of this tensor are positive so the following relation must be satisfied [32–34]:

$$k_{ii}k_{jj} > k_{ij} \quad for \quad i \neq j \tag{2b}$$

Using the Clausius_Duhem inequality, the following inequalities for the conductive coefficients of orthotropic materials are achieved:

$$k_{(ii)} \geqslant 0 \tag{2c}$$

$$\frac{1}{2}(k_{(ii)}k_{(jj)} - k_{(ji)}k_{(ij)}) \geqslant 0 \tag{2d}$$

$$\varepsilon_{ijk}k_{(1j)}k_{(2j)}k_{(3j)\geqslant 0} \tag{2e}$$

where k_{ij} represents the symmetric part of tensor:

$$k_{(ij)} = k_{(ji)} = \frac{k_{ij}+k_{ji}}{2} \tag{2f}$$

These relations are valid in all coordinate systems. Two separate coordinate systems must be considered to investigate heat transfer problems in composite laminates: "on-axis" coordinate system (x_1, x_2, x_3) and "off-axis" coordinate system (r, ϕ, θ) [35]. The direction of the "on axis" coordinate depends on the fibers' orientation in each layer: x_1 is parallel to fiber, x_2 is perpendicular to fiber in layer and x_3 is perpendicular to layer. Since composite materials are generally fabricated by laying layers on top of each other, the fiber orientation may differ between layers. We need to define an off axis coordinate system to study the physical properties in unique directions. Thus, there is an angular deviation between the on axis and off axis coordinates. The Fourier equation in on-axis coordinate will be [36]:

$$\begin{pmatrix} q_r \\ q_\theta \\ q_\phi \end{pmatrix} = -\begin{pmatrix} k_{11} & 0 & 0 \\ 0 & k_{22} & 0 \\ 0 & 0 & k_{33} \end{pmatrix} \begin{pmatrix} \frac{\partial T}{\partial r} \\ \frac{1}{r}\frac{\partial T}{\partial \theta} \\ \frac{1}{r\sin\theta}\frac{\partial T}{\partial \phi} \end{pmatrix} \tag{3}$$

The off-axis conductivity tensor $[\bar{k}]$ is obtained by applying the rotation θ to the on-axis conductivity tensor $[k]$:

$$[\bar{k}] = T(\theta)[k]T(-\theta) \tag{4}$$

where $T(\theta)$ is the rotation tensor [28]:

$$T(\theta) = \begin{bmatrix} \cos(\theta) & -\sin(\theta) & 0 \\ \sin(\theta) & \cos(\theta) & 0 \\ 0 & 0 & 1 \end{bmatrix} \tag{5}$$

The heat conduction coefficients can be directly obtained from experimental measurements or be calculated based on the theoretical models [36–46].

3. Modeling and Formulations

In this section, governing equation of heat conduction in spherical composite is presented and general boundary conditions used in this study are introduced. Fibers' direction can be varied in each layer (see Fig. 1) and (r, ϕ, θ) are the off-axis coordinates. Applying the balance of energy in element of sphere which has shown in Fig. 2, the following equation will be achieved:

$$\frac{\partial q_\phi dA_\phi}{\partial\phi}d\phi+\frac{\partial q_\theta dA_\theta}{\partial\theta}d\theta+\frac{\partial q_r dA_r}{\partial r}dr=\rho c_p\frac{\partial T}{\partial t}dv \tag{7}$$

Surface areas and volume of sphere element are as follows:

$$\begin{aligned} dA_r &= r^2\sin\theta d\phi d\theta \\ dA_\theta &= r\sin\theta d\phi d\theta \\ dA_\phi &= rd\theta dr \\ dv &= r^2\sin\theta dr d\phi d\theta \end{aligned} \tag{8}$$

Quantities ρ and c_p in Eq. (7) are the density and specific heat capacity at constant pressure, respectively. Substituting Eq. (1) and Eq. (8) into Eq. (7) will be resulted in:

$$\begin{aligned} &\bar{k}_{11}\frac{1}{r^2}\frac{\partial}{\partial r}\left(r^2\frac{\partial T}{\partial r}\right)+\bar{k}_{22}\frac{1}{r^2\sin\theta}\frac{\partial^2 T}{\partial\Phi^2}+\bar{k}_{33}\frac{1}{r^2\sin\theta}\frac{\partial}{\partial\theta}\left(\sin\theta\frac{\partial T}{\partial\theta}\right) \\ &\quad+\frac{(\bar{k}_{12}+\bar{k}_{21})}{r\sin\theta}\frac{\partial^2 T}{\partial r\partial\phi}+\bar{k}_{12}\frac{1}{r^2\sin\theta}\frac{\partial T}{\partial\Phi}+\frac{(\bar{k}_{13}+\bar{k}_{31})}{r}\frac{\partial^2 T}{\partial r\partial\theta}+\bar{k}_{13} \\ &\quad\times\frac{1}{r^2}\frac{\partial T}{\partial\theta}+(\bar{k}_{32}+\bar{k}_{23})\frac{1}{r^2\sin\theta}\frac{\partial^2 T}{\partial\theta\partial\Phi}+\bar{k}_{31}\frac{\cos\theta}{r\sin\theta}\frac{\partial T}{\partial r} \\ &\quad=\rho C_p\frac{\partial T}{\partial t} \end{aligned} \tag{9}$$

Here, steady-state conductive heat transfer in the r and θ directions are considered. Thus, Eq. (9) can be simplified to

$$\bar{k}_{11}\frac{1}{r^2}\frac{\partial}{\partial r}\left(r^2\frac{\partial T}{\partial r}\right)+\bar{k}_{22}\frac{1}{r^2\sin\theta}\frac{\partial}{\partial\theta}\left(\sin\theta\frac{\partial T}{\partial\theta}\right)=0 \tag{10}$$

The off-axis component of conductivity tensor ($\bar{k}_{11}$ and $\bar{k}_{22}$) are obtained by substituting Eq. (5) into Eq. (4):

$$\begin{cases} k_{11}{}^{-}=k_{22} \\ k_{22}{}^{-}=m_l^2k_{11}+n_l^2k_{22}, \quad m_l=\cos\Psi_i,\ n_l=\sin\Psi_i \end{cases} \tag{11}$$

where Ψ is the angle between the tangent line to fibers and θ direction as shown schematically in Fig. 1. Substituting the determined off-axis coefficients (Eq. (11)) into energy equation (Eq. (10)) results:

$$\frac{1}{r^2}\frac{\partial}{\partial r}\left(r^2\frac{\partial T}{\partial r}\right)+\frac{1}{\mu_i^2}\frac{1}{r^2\sin\theta}\frac{\partial}{\partial\theta}\left(\sin\theta\frac{\partial T}{\partial\theta}\right)=0 \tag{12}$$

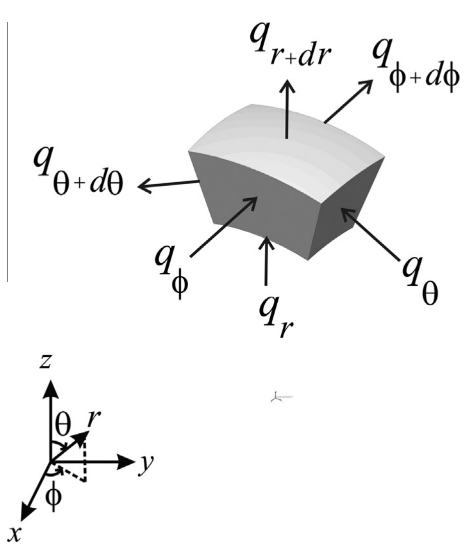

Fig. 2. Schematic of heat fluxes on a spherical element.

where parameter μ_i is given by:

$$\mu_i=\sqrt{\frac{k_{22}}{m_l^2k_{11}+n_l^2k_{22}}} \tag{13}$$

It is important to mention that μ_i can be changed layer by layer and so the energy equation will be change in each layer; this fact leads to different temperature distribution in layers. In order to connect the different temperature distributions in each layer, continuity of temperature and heat flux in margin of each pair of layers must be considered as follows:

$$T^{(i)}-T^{(i+1)}=0 \tag{14a}$$

$$k_{22}^{(i)}\frac{\partial T^{(i)}}{\partial r}-k_{22}^{(i+1)}\frac{\partial T^{(i+1)}}{\partial r}=0 \tag{14b}$$

The general linear boundary conditions inside and outside of the sphere are in the following forms which can covers wide range of applicable thermal conditions:

$$a_1T(r_0,\theta)+b_1\frac{\partial T}{\partial r}(r_0,\theta)=f_1(\theta) \tag{15a}$$

$$a_2T(r_{nl},\theta)+b_2\frac{\partial T}{\partial r}(r_{nl},\theta)=f_2(\theta) \tag{15b}$$

Note that $f_1(\theta)$, $f_2(\theta)$ are the arbitrary functions, the constant a_1, a_2 have the same dimension as convection coefficient and b_1, b_2 have the same dimension as conduction coefficient.

4. Analytical solution under general boundary conditions

In this section, the analytical solution of steady temperature distribution under generalized linear boundary conditions is presented based on separation of variables method. By applying the separation of variables method on Eq. (12), the temperature distribution could be separated as two independent functions $R(r)$ and $\Theta(\theta)$:

$$T(r,\theta)=R(r)\Theta(\theta) \tag{16}$$

Substituting Eq. (16) into the Eq. (12), heat conduction equation has been separated as:

$$\left(r^2\frac{R''}{R}+2r\frac{R'}{R}\right)=-\frac{1}{\mu^2}\left(\frac{\cos\theta}{\sin\theta}\frac{\dot{\Theta}}{\Theta}+\frac{\ddot{\Theta}}{\Theta}\right)=\lambda \tag{17}$$

where λ is a constant. By supposing $x=\sin\theta$, the separated equation in θ direction can be solved as a Legendre equation:

$$\frac{\partial}{\partial x}\left(1-x^2\frac{\partial\Theta}{\partial x}\right)+n(n+1)\Theta=0 \tag{18}$$

The solution of Eq. (18) is as follows [47]:

$$\Theta(\theta)=\sum_{n=0}^{\infty}A_nP_n(\cos\theta) \tag{19}$$

where P_n indicates the Legendre function of degree n and order one, and A_n is the coefficient of Legendre series. Comparing Eqs. (17) and (18), λ will be achieved as follows:

$$\lambda=\frac{n(n+1)}{\mu^2} \tag{20}$$

According to Eq. (17), the separated equation in r direction is an Euler equation with the underneath solution:

$$R_n(r)=\begin{cases} B_nr^{\frac{n}{\mu^2}}+C_nr^{\frac{-(n+1)}{\mu^2}} & \textit{for } n\geqslant 1 \\ B_0\ln r+C_0 & \textit{for } n=0 \end{cases} \tag{21}$$

The temperature distribution in each layer will be:

$$T^{(i)}(r,\theta)=\left(a_0^{(i)}\ln\left(\frac{r}{r_{nl}}\right)+b_0^{(i)}\right)P_0(\cos\theta)+\sum_{n=1}^{\infty}\left(a_n^{(i)}\left(\frac{r}{r_{nl}}\right)^{\frac{n}{\mu^2}}+b_n^{(i)}\left(\frac{r}{r_{nl}}\right)^{\frac{-(n+1)}{\mu^2}}\right)P_n(\cos\theta) \quad (22)$$

where index i refer to the number of layers and the following relations are existed for coefficients of above temperature distribution:

$$\begin{aligned} a_\chi^{(i)}&=A_\chi^{(i)}B_\chi^{(i)} \\ b_\chi^{(i)}&=A_\chi^{(i)}C_\chi^{(i)} \end{aligned}\quad \chi=0,n \quad (23)$$

Finally, by applying the inside and outside boundary conditions in the direction of r and applying the continuity of temperature and heat flux at the boundary located between layers, the coefficients a_0, b_0, a_n, b_n are obtained as follows:

- By applying boundary condition inside and outside of sphere Eqs. (15a) and (15b), we have:

$$\left(\left(a_1\ln\left(\frac{r_0}{r_{nl}}\right)+b_1\left(\frac{1}{r_0}\right)\right)a_0^{(1)}+a_1b_0^{(1)}\right)P_0(\cos\theta)+\left(\begin{array}{c}\left(a_1r_0^{\frac{n}{\mu_m^2}}+b_1\frac{n}{\mu_0^2}r_0^{\frac{n}{\mu_0^2}-1}\right)a_n^{(1)}+\\ \left(a_2r_0^{\frac{-(n+1)}{\mu_0^2}}+b_2\frac{-(n+1)}{\mu_0^2}r_0^{\frac{-(n+1)}{\mu_0^2}-1}\right)b_n^{(1)}\end{array}\right)P_n(\cos\theta)=f_1(\theta) \quad (24a)$$

$$\left(\frac{b_2}{r_{nl}}a_0^{(n_l)}+a_2b_0^{(n_l)}\right)P_0(\cos\theta)+\sum_{n=1}^{\infty}\left(\begin{array}{c}\left(a_2r_{nl}^{\frac{n}{\mu_{n_l}^2}}+b_2\frac{n}{\mu_m^2}r_{nl}^{\frac{n}{\mu_{n_l}^2}-1}\right)a_n^{(n_l)}+\\ \left(a_2r_{nl}^{\frac{-(n+1)}{\mu_{n_l}^2}}+b_2\frac{-(n+1)}{\mu_{n_l}^2}r_{nl}^{\frac{-(n+1)}{\mu_{n_l}^2}-1}\right)b_n^{(n_l)}\end{array}\right)P_n(\cos\theta)=f_2(\theta) \quad (24b)$$

- The following equations could be expressed by applying the temperature and the heat flux continuity at the boundary located between the layer i and $i+1$ (Eqs. (14a) and (14b)):

$$\left(\ln\left(\frac{r_i}{r_{nl}}\right)a_0^{(i)}+b_0^{(i)}-\ln\left(\frac{r_i}{r_{nl}}\right)a_0^{(i+1)}+b_0^{(i+1)}\right)P_0(\cos\theta)+\sum_{n=1}^{\infty}\left(\begin{array}{c}\left(\frac{r_i}{r_{nl}}\right)^{\frac{n}{\mu_i^2}}a_n^{(i)}+\left(\frac{r_i}{r_{nl}}\right)^{\frac{-(n+1)}{\mu_i^2}}b_n^{(i)}-\\ \left(\frac{r_i}{r_{nl}}\right)^{\frac{n}{\mu_{i+1}^2}}a_n^{(i+1)}-\left(\frac{r_i}{r_{nl}}\right)^{\frac{-(n+1)}{\mu_{i+1}^2}}b_n^{(i+1)}\end{array}\right)P_n(\cos\theta)=0 \quad (24c)$$

$$\left(\left(\frac{1}{r_{nl}}\right)\ln\left(\frac{r_i}{r_{nl}}\right)a_0^{(i)}-\left(\frac{1}{r_{nl}}\right)\ln\left(\frac{r_i}{r_{nl}}\right)a_0^{(i+1)}\right)P_0(\cos\theta)+\sum_{n=1}^{\infty}\left(\begin{array}{c}\frac{n}{\mu_i^2}\left(\frac{r_i}{r_{nl}}\right)^{\frac{n}{\mu_i^2}-1}a_n^{(i)}-\frac{(n+1)}{\mu_i^2}\left(\frac{r_i}{r_{nl}}\right)^{\frac{-(n+1)}{\mu_i^2}-1}b_n^{(i)}-\\ \frac{n}{\mu_{i+1}^2}\left(\frac{r_i}{r_{nl}}\right)^{\frac{n}{\mu_{i+1}^2}-1}a_n^{(i+1)}+\frac{(n+1)}{\mu_{i+1}^2}\left(\frac{r_i}{r_{nl}}\right)^{\frac{-(n+1)}{\mu_{i+1}^2}-1}b_n^{(i+1)}\end{array}\right)P_n(\cos\theta)=0 \quad (24d)$$

Using the existing relations for orthogonal Legendre functions [47,48] and rearranging the Eqs. (24a) to (24d), the unknown coefficients will be achieved.

- Resorting Eq. (24a) results:

$$\begin{aligned}&\left(a_1\ln\left(\frac{r_0}{r_{nl}}\right)+b_1\left(\frac{1}{r_0}\right)\right)a_0^{(1)}+a_1b_0^{(1)}=F_0^0,\\ &\left(a_1r_0^{\frac{n}{\mu_m^2}}+b_1\frac{n}{\mu_0^2}r_0^{\frac{n}{\mu_0^2}-1}\right)a_n^{(1)}+\left(a_2r_0^{\frac{-(n+1)}{\mu_0^2}}+b_2\frac{-(n+1)}{\mu_0^2}r_0^{\frac{-(n+1)}{\mu_0^2}-1}\right)b_n^{(1)}\\ &=F_n^0\end{aligned} \quad (25a)$$

- Similarly, Eq. (24b) results:

$$\begin{aligned}&\frac{b_2}{r_{nl}}a_0^{(n_l)}+a_2b_0^{(n_l)}=F_0^{n_l}\\ &\left(a_2r_{nl}^{\frac{n}{\mu_m^2}}+b_2\frac{n}{\mu_m^2}r_{nl}^{\frac{n}{\mu_m^2}-1}\right)a_n^{(n_l)}+(a_2r_{nl}^{\frac{-(n+1)}{\mu_m^2}}\\ &\quad+b_2\frac{-(n+1)}{\mu_m^2}r_{nl}^{\frac{-(n+1)}{\mu_m^2}-1})b_n^{(n_l)}=F_n^{n_l}\end{aligned} \quad (25b)$$

where

$$\begin{aligned}&F_\chi^0=\frac{2n+1}{2}\int_0^\pi f_1(\theta)P_\chi(\cos(\theta))\sin(\theta)d\theta\\ &\chi=0,nF_\chi^{n_l}=\frac{2n+1}{2}\int_0^\pi f_2(\theta)P_\chi(\cos(\theta))\sin(\theta)d\theta\end{aligned} \quad (25c)$$

- Also, regarding to the Eq. (24c):

$$\begin{aligned}&\left(\ln\left(\frac{r_i}{r_{nl}}\right)a_0^{(i)}+b_0^{(i)}-\ln\left(\frac{r_i}{r_{nl}}\right)a_0^{(i+1)}+b_0^{(i+1)}\right)=0\\ &\left(\frac{r_i}{r_{nl}}\right)^{\frac{n}{\mu_i^2}}a_n^{(i)}+\left(\frac{r_i}{r_{nl}}\right)^{\frac{-(n+1)}{\mu_i^2}}b_n^{(i)}-\left(\frac{r_i}{r_{nl}}\right)^{\frac{n}{\mu_{i+1}^2}}a_n^{(i+1)}-\left(\frac{r_i}{r_{nl}}\right)^{\frac{-(n+1)}{\mu_{i+1}^2}}b_n^{(i+1)}=0\end{aligned} \quad (25d)$$

- Rearranging the Eq. (24d) results:

$$\begin{aligned}&\left(\left(\frac{1}{r_{nl}}\right)\ln\left(\frac{r_i}{r_{nl}}\right)a_0^{(i)}-\left(\frac{1}{r_{nl}}\right)\ln\left(\frac{r_i}{r_{nl}}\right)a_0^{(i+1)}\right)=0,\\ &\frac{n}{\mu_i^2}\left(\frac{r_i}{r_{nl}}\right)^{\frac{n}{\mu_i^2}-1}a_n^{(i)}-\frac{(n+1)}{\mu_i^2}\left(\frac{r_i}{r_{nl}}\right)^{\frac{-(n+1)}{\mu_i^2}-1}b_n^{(i)}-\frac{n}{\mu_{i+1}^2}\left(\frac{r_i}{r_{nl}}\right)^{\frac{n}{\mu_{i+1}^2}-1}a_n^{(i+1)}\\ &+\frac{(n+1)}{\mu_{i+1}^2}\left(\frac{r_i}{r_{nl}}\right)^{\frac{-(n+1)}{\mu_{i+1}^2}-1}b_n^{(i+1)}=0\end{aligned} \quad (25e)$$

Eqs. (25a), (25b), (25d) and (25e) should be solved to determine the coefficients $a_n^{(i)}$ and $b_n^{(i)}$. The coefficients of this set of equations form a five diagonal matrix. In this study, Thomas algorithm is used to find these coefficients analytically. According to this algorithm, the reciprocity relations for calculating $a_n^{(i)}$ and $b_n^{(i)}$ are given as follows:

$$\begin{aligned}&b_\chi^{(n_l)}=\gamma^{2n_l}\\ &\begin{cases}a_\chi^{(i)}=\gamma^{2i-1}-b_\chi^{(i)}\beta_i\\ b_\chi^{(i-1)}=\gamma^{2i-2}-a_\chi^{(i)}\alpha_i\end{cases}\quad i=n_l,n_l-1,\ldots,2\\ &a_\chi^{(1)}=\gamma^1-b_\chi^{(1)}\beta_1\end{aligned} \quad (26)$$

The index χ could be *0* or n to cover all unknown coefficients. The relations related to α, β and γ in each value of χ are available in appendix.

5. Results and discussion

In this section, the ability of the presented analytical solution is examined by applying it to solving two industrial applications: a multilayer spherical composite vessel under varying sun heat flux and a multi-layer composite spherical shell with varying inside

Table 1
Composite polymer properties [49].

Material number	Filler	Matrix	k_{11} (W/mK)	k_{22} (W/mK)	Density (g/cc)	Wt. (%) filler
1	Thermal Graph DKD X	Lexan HF 110-11 N	11.4	0.74	1.46	40
2	Thermal Graph DKD X	Lexan HF 110-11 N	8	0.6	1.38	30
3	Thermocarb CF300	Zytel 110 NC010	1.1	0.4	1.17	5

temperature. Thermal properties of composite materials which are used in this study are presented in Table 1. In order to investigate the effects of fibers' angle on heat conduction and temperature distribution of laminates, four common arrangements of fibers in laminate have been considered:

- **Isotropic:** Fibers in whole of laminate are in ϕ direction. (Fibers' angles in each laminas are equal to 90°). The composite laminate is in form of an isotropic spherical laminate with conductive coefficients $k_{rr} = k_{\theta\theta} = k_{22}$.
- **Orthotropic:** Fibers in whole of laminate are in θ direction. (Fibers' angles in each laminas are equal to zero). The composite laminate is such as a block orthotropic material with conductive coefficients $k_{\theta\theta} = k_{11}$ and $k_{rr} = k_{22}$.
- **Cross-ply:** Fibers' angle is [0°, 90°, 0°, 90°, ...].
- **[0°, 45°, 90°, 135°, ...]:** An intermediate arrangement that the fibers' angle change 45° in each layer.

An analytical solution for two-dimension steady heat conduction in a single layer isotropic spherical laminate has been presented by Arpaci [47]. Arpaci solution is simple part of current research that the angle of fibers' in a single-layer laminate is equal to. The result of Arpaci solution is used to investigate the validation of present analytical solution. As shown in Fig. 3, the result for the current solution agrees completely with the analytical solution of Arpaci [47]. Here, because of the strong convergence of the temperature Fourier series, calculating the first ten terms of them is sufficient.

- **Case 1: Multi-layer spherical composite vessel**

Heat conduction in a three-layer vessel with varying heat flux at outside has been considered. It is considered that sun radiation heat flux varied as $q'' = q_\circ(1 + \cos(\theta/2))$, where $q_\circ$ is average of sun heat flux on earth and is considered equal to 1357 W/m^2 [50]. It is assumed that the vessel is cooled with air. Fig. 4 shows the geometry and boundary conditions of this vessel. Table 2 presents the properties of this vessel. The inner surface temperature is assumed to be constant.

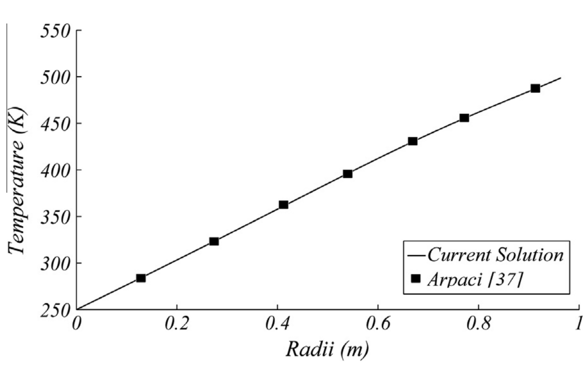

Fig. 3. Temperature distribution of an isotropic sphere in radial direction (T_{out} = 500 K, r_{out} = 1 m, θ = 45°).

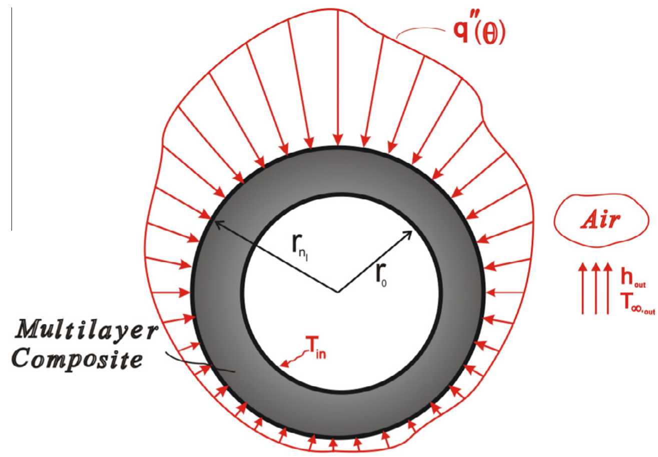

Fig. 4. Geometry and boundary conditions of composite spherical vessel.

Table 2
Geometry and boundary conditions of composite spherical vessel.

Inner diameter (cm)	100
Outer diameter (cm)	130
Thickness of each layer (cm)	5
Ambient temperature (K)	310
Internal temperature (K)	300
Convective coefficient (W/m^2 K)	100

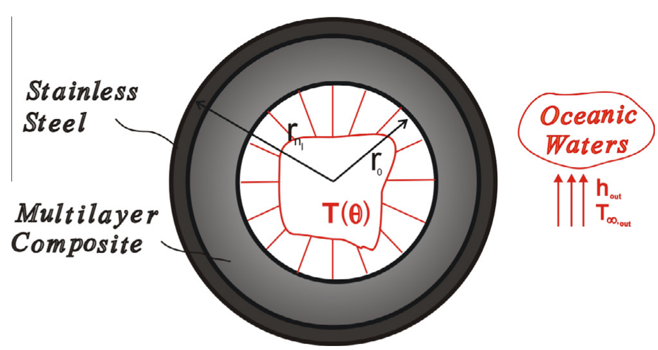

Fig. 5. Geometry and boundary conditions of composite spherical shell.

Table 3
Geometry and boundary conditions of composite spherical shell.

Inner diameter (cm)	50
Outer diameter (cm)	62
Thickness of each layer (cm)	1
Ambient temperature (K)	283
Convective coefficient (W/m^2 K)	500

- **Case 2: Multi-layer spherical composite shell**

Heat conduction through a composite spherical shell is considered as the second example. This laminate is used for storing radioactive wastes in oceanic waters [51]. It is supposed that this spherical shell is made of a five-layer composite with a stainless steel layer outside of sphere. The inner temperature of sphere is considered to vary in the form of $T(\theta) = 300(1 + \cos(\theta))$ for more complexity of boundary conditions. Convective heat transfer has been applied as the second radial boundary condition. The geometry and boundary conditions of tank are presented in Fig. 5 and Table 3.

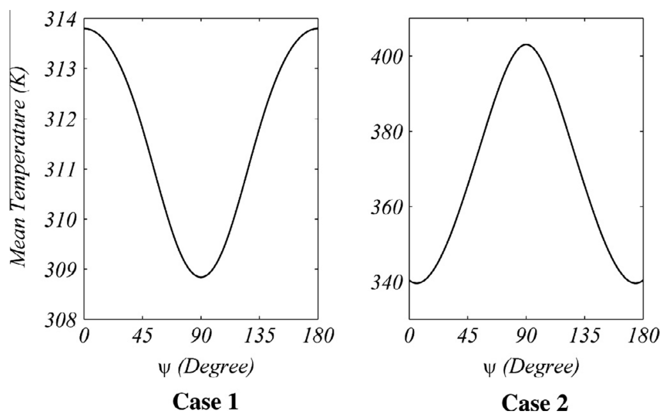

Fig. 6. Mean temperature of laminates for composite spherical vessel and shell cases.

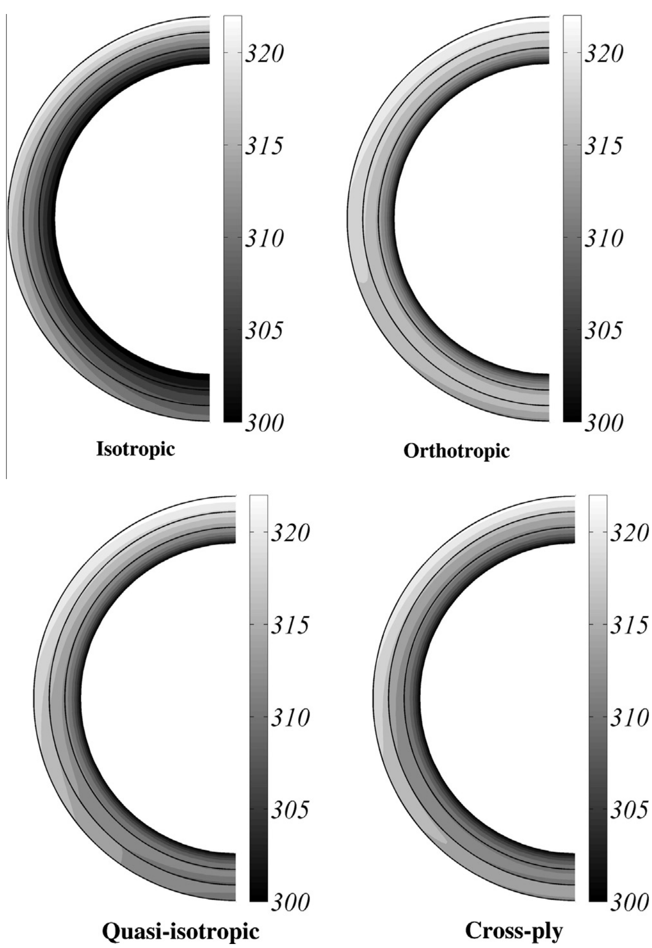

Fig. 7. Contours of temperature distribution in r and θ directions at different arrangements of fibers for the composite spherical vessel case.

Fig. 6 shows the variation of mean temperature of laminate versus fibers' angle for two mentioned cases. It is supposed that the fibers' angle in all laminates is similar and vary with each other. For the first case, mean temperature of laminate has been increased with growth of cone angle from 0° to 90°. Unlike the

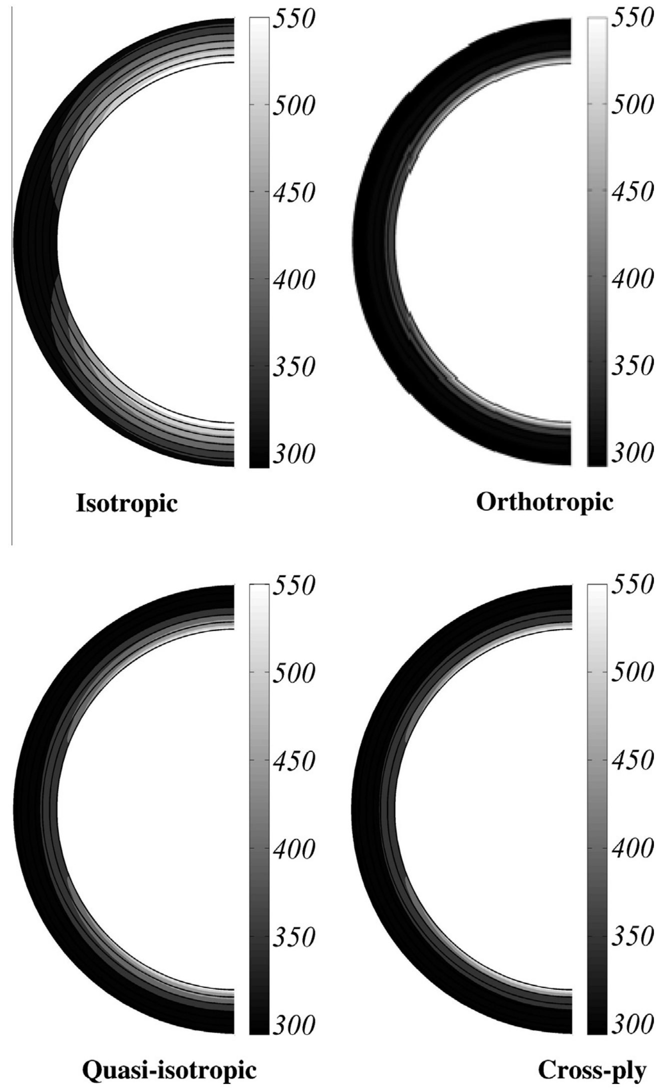

Fig. 8. Contours of temperature distribution in r and θ directions at different arrangements of fibers for the composite spherical shell case.

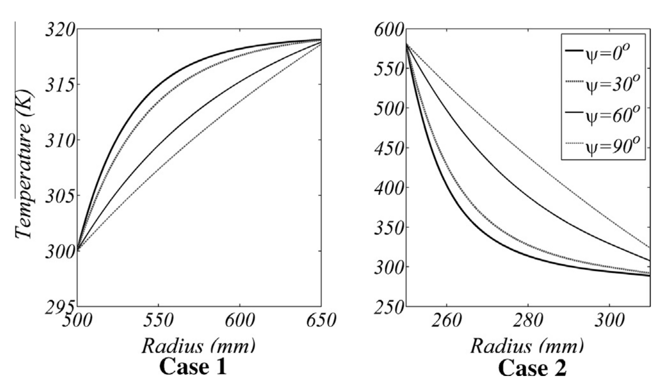

Fig. 9. Temperature distribution of laminates in r direction under different cone angle for composite spherical vessel and shell cases.

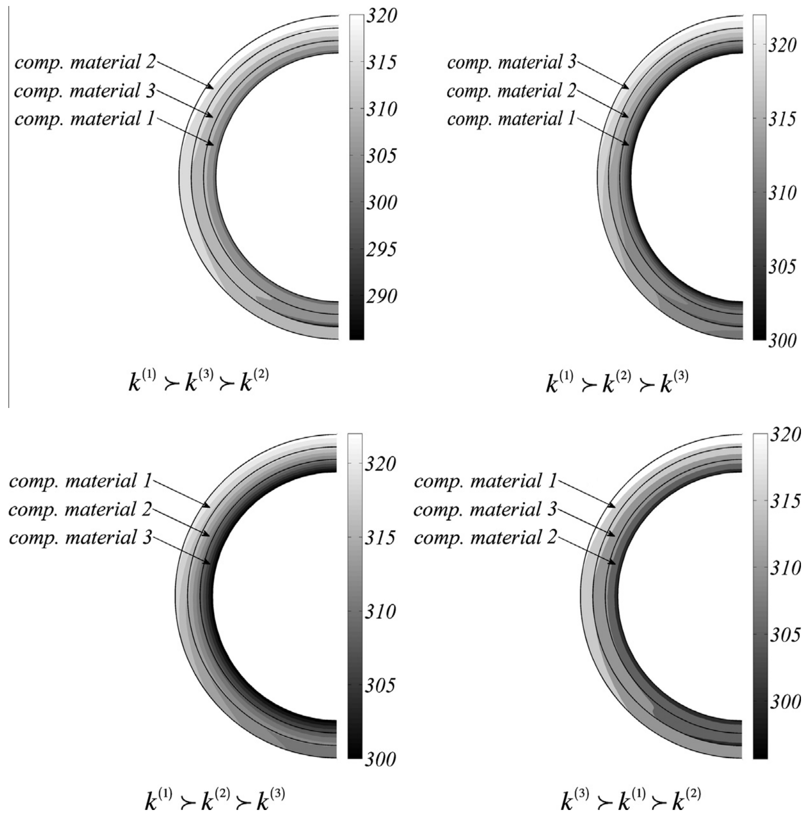

Fig. 10. Contours of temperature distribution in r and θ directions at different arrangements of composite materials for the composite spherical vessel case.

second case, increasing cone angle results decreasing of mean temperature; this contrast is because of different outside/inside thermal boundary conditions.

Contours 7 and 8 depicted the temperature distribution in different fiber arrangements of spherical composite laminates for case 1 and case 2, respectively. According to the figures, fiber arrangement has a significant effect on temperature distribution pattern in both cases. Respect to application and thermal conditions of design, the best arrangement of fibers in laminate should be selected (see Fig. 7 and 8).

Fig. 9 shows the variation of temperature in radial direction in a specific cone angle for case 1 and case 2, respectively. Here, it is assumed that the fibers' angle is equal in whole of laminate. According to the figure, when the cone angle, Ψ, is 90°, the temperature's gradient is as an isotropic material. On the other hand, when cone angle far from 90° and near to 0°, the thermal behavior of composite changed more and more until orthotropic behavior appears in $\Psi = 0°$.

Fig. 10 shows the effect of layer material arrangements on temperature distribution for case 1. According to the figure, the sequence of composite materials in laminate could change the temperature distribution pattern in laminate greatly and should be considered as an important factor in multilayer composite materials.

6. Conclusions

In present paper, an exact analytical solution for steady conductive heat transfer in spherical laminates is presented as the first time. The solution is obtained under general linear boundary conditions so it could be applied simplicity for various conditions including combinations of conduction, convection, and radiation both inside and outside of the sphere. The results of present study is useful for analyzing of thermal fracture, controlling directional heat transfer through laminates and fiber placement in production processes of spherical vessels. Here, we examined the capability of the present solution by applying it on two industrial applications for different fiber arrangement of multilayer spherical laminates. The analytical solution indicated that the temperature distribution for any arbitrary fiber arrangement will be intermediate between those in single-layer laminates with fiber angles of 0% and 90%. The authors suggest that the future works could be focused on unsteady and non-Fourier heat conduction in spherical laminates.

Acknowledgments

This paper is presented based on a researching project which is Granted by Shahrood University of Technology. Therefore, the authors appreciate for their financial support.

Appendix A. The coefficients of temperature distribution

In this section, the relations of coefficients of temperature distribution of any lamina are presented:

$$\begin{cases} \beta_1 = \frac{B_\chi^0}{A_\chi^0} \\ \gamma^1 = F_\chi^0 \times \beta_1 \end{cases} \tag{A1}$$

$$\begin{cases} \alpha_{i+1} = \frac{-A_\chi^{i+1} + B_\chi^{i+1} \times (\xi_i)}{(B_\chi^i + B_\chi^{i+1} \times (\tau_i) - A_\chi^i \times \beta_i)} \\ \gamma^{2i} = -\gamma^{2i-1} \times A_\chi^i \times \alpha_{i+1} \end{cases} \quad i = 1, 2, 3, \ldots, n_l - 1 \tag{A2}$$

$$\begin{cases} \beta_{i+1} = \frac{1}{(\xi_i) - \alpha_{i+1} \times (\tau_i)} \\ \gamma^{2i+1} = -\gamma^{2i} \times B_\chi^{\prime i} \times \beta_{i+1} \end{cases} \quad i = 1, 2, 3, \ldots, n_l - 1 \tag{A3}$$

Coefficients ξ_i and τ_i are defined for simplicity:

$$\begin{cases} \xi_i = \frac{A'^{i}_{\chi} \times A^{i+1}_{\chi} - A^{i}_{\chi} \times A'^{i+1}_{\chi}}{A'^{i}_{\chi} \times B^{i+1}_{\chi} - A^{i}_{\chi} \times B'^{i+1}_{\chi}} \\ \tau_i = \frac{-A'^{i}_{\chi} \times B^{i}_{\chi} + A^{i}_{\chi} \times B'^{i}_{\chi}}{A'^{i}_{\chi} \times B^{i+1}_{\chi} - A^{i}_{\chi} \times B'^{i+1}_{\chi}} \end{cases} \quad i = 1, 2, 3, \ldots, n_l - 1 \tag{A4}$$

The values of coefficients A_χ and B_χ related to each pair of coefficients are as follows (the coefficients A'_χ and B'_χ are the derivative of A_χ and B_χ, respectively):

$$\begin{cases} A_0^0 = a_1 \ln\left(\frac{r_0}{r_{nl}}\right) + b_1\left(\frac{1}{r_0}\right), A_n^0 = a_1 r_0^{\frac{n}{\mu_m^2}} + b_1 \frac{n}{\mu_0^2} r_0^{\frac{n}{\mu_0^2}-1} \\ B_0^0 = a_1, B_{1n}^0 = a_2 r_0^{\frac{-(n+1)}{\mu_0^2}} + b_2 \frac{-(n+1)}{\mu_0^2} r_0^{\frac{-(n+1)}{\mu_0^2}-1} \\ A_0^i = \ln\left(\frac{r_i}{r_{nl}}\right), A_{1n}^i = \left(\frac{r_i}{r_{nl}}\right)^{\frac{n}{\mu_i^2}} \\ B_0^i = 1, B_{1n}^i = \left(\frac{r_i}{r_{nl}}\right)^{\frac{-(n+1)}{\mu_i^2}} \\ A_0^{n_l} = \frac{b_2}{r_{nl}}, A_n^{n_l} = a_2 r_{nl}^{\frac{n}{\mu_{n_l}^2}} + b_2 \frac{n}{\mu_{n_l}^2} r_{nl}^{\frac{n}{\mu_{n_l}^2}-1} \\ B_0^{n_l} = a_2, B_n^{n_l} = a_2 r_{nl}^{\frac{-(n+1)}{\mu_{n_l}^2}} + b_2 \frac{-(n+1)}{\mu_{n_l}^2} r_{nl}^{\frac{-(n+1)}{\mu_{n_l}^2}-1} \end{cases} \quad i = 1, 2, 3, \ldots, n_l - 1 \tag{A5}$$

References

[1] Barrett DJ. The mechanics of z-fiber reinforcement. Compos Struct 1996;36:23–32.

[2] Mair RI. Advanced composite structures research in Australia. Compos Struct 2002;57:3–10.

[3] Chao CK, Che FM, Shen MH. An exact solution for thermal stresses in a three-phase composite cylinder under uniform heat flow. Int J Solids Struct 2007;44:926–40.

[4] Xiao JR, Gilhooley DF, Batra RC, Gillespie Jr JW, McCarthy MA. Analysis of thick composite laminates using a higher-order shear and normal deformable plate theory (HOSNDPT) and a meshless method. Composites: Part B 2008;39: 414–27.

[5] Pradeep V, Ganesan N. Thermal buckling and vibration behavior of multi-layer rectangular viscoelastic sandwich plates. J Sound Vibrat 2008;310:169–83.

[6] Papargyris DA, Day RJ, Nesbitt A, Bakavos D. Comparison of the mechanical and physical properties of a carbon fiber epoxy composite manufactured by resin transfer molding using conventional and microwave heating. Compos Sci Technol 2008;68:1854–61.

[7] Topal U, Uzman U. Thermal buckling load optimization of laminated composite plates. Thin Walled Struct 2008;46:667–75.

[8] Ootao Y, Tanigawa Y. Transient thermal stresses of angle-ply laminated cylindrical panel due to nonuniform heat supply in the circumferential direction. Compos Struct 2002;55:95–103.

[9] Ju DY. Simulation of thermo-mechanical behavior and interfacial stress of metal matrix composite under thermal shock process. Compos Struct 2000;48: 113–8.

[10] Ding Y, Chiu WK, Liu XL, Whittingham B. Modeling of thermal response of oil-heated tools due to different flow rates for the manufacture of composite structures. Compos Struct 2001;54:477–88.

[11] Shojaei A, Ghaffarian SR, Karimian SMH. Three-dimensional process cycle simulation of composite parts manufactured by resin transfer molding. Compos Struct 2004;65:381–90.

[12] Blanc M, Touratier M. An efficient and simple refined model for temperature analysis in thin laminated composites. Compos Struct 2007;77:193–205.

[13] Miller JR, Weaver PM. Temperature profiles in composite plates subject to time-dependent complex boundary conditions. Compos Struct 2003;59: 267–78.

[14] Hsieh MH, Ma CC. Analytical investigations for heat conduction problems in anisotropic thin-layer media with embedded heat sources. Int J Heat Mass Transfer 2002;45:4117–32.

[15] Ma CC, Chang SW. Analytical exact solutions of heat conduction problems for anisotropic multi-layered media. Int J Heat Mass Transfer 2004;47:1643–55.

[16] SALT H. Transient conduction in a two-dimensional composite slab-I. Theoretical development of temperature modes. Int J Heat Mass Transfer 1983;26:1611–6.

[17] SALT H. Transient conduction in a two-dimensional composite slab-II. Physical interpretation of temperature modes.. Int J Heat Mass Transfer 1983;26: 1617–23.

[18] de Monte F. Transient heat conduction in one-dimensional composite slab. A 'natural' analytic approach. Int J Heat Mass Transfer 2000;43:3607–19.

[19] de Monte F. An analytic approach to the unsteady heat conduction processes in one-dimensional composite media. Int J Heat Mass Transfer 2002;45:1333–43.

[20] de Monte F. Unsteady heat conduction in two-dimensional two slab-shaped regions. Exact closed-form solution and results. Int J Heat Mass Transfer 2003; 46:1455–69.

[21] de Monte F. Multi-layer transient heat conduction using transition time scales. Int J Therm Sci 2006;45:882–92.

[22] Kayhani MH, Norouzi M, Amiri Delouei A. A general analytical solution for heat conduction in cylindrical multilayer composite laminates. Int J Therm Sci 2012;52:73–82.

[23] Kayhani MH, Norouzi M, Amiri Delouei A. An exact solution of axi-symmetric conductive heat transfer in cylindrical composite laminate under the general boundary condition. Word Acad Sci Eng Technol 2010;69:55–62.

[24] Kayhani MH, Norouzi M, Amiri Delouei A. On heat conduction problem in multi–layer composite pin fins. In: Proceedings of third international conference of advanced composite materials engineering (COMAT), Brasov, Romani; 2010. p. 89–94.

[25] Amiri Delouei A, Kayhani MH, Norouzi M. Exact analytical solution of unsteady axi-symmetric conductive heat transfer in orthotropic cylindrical composite laminates. Int J Heat Mass Transfer 2012;55:4427–36.

[26] Tarn JQ. Exact solution for functionally graded anisotropic cylinders subjected to thermal and mechanical loads. Solids Struct 2001;38:8189–206.

[27] Tarn JQ, Wang YM. End effects of heat conduction in circular cylinders of functionally graded materials and laminated composites. Int J Heat Mass Transfer 2004;47:5741–7.

[28] Kayhani MH, Shariati M, Norouzi M, Karimi Demneh M. Exact solution of conductive heat transfer in cylindrical composite laminate. Heat Mass Transfer 2009;46:83–94.

[29] Norouzi M, Rezaei Niya SM, Kayhani MH, Karimi Demneh M, Naghavi MS. Exact solution of unsteady conductive heat transfer in cylindrical composite laminates. J Heat Transfer (ASME) 2012;134:101301.

[30] Singh S, Jain PK, Rizwan-uddin. Analytical solution to transient heat conduction in polar coordinates with multiple layers in radial direction. Int J Therm Sci 2008;47:261–73.

[31] Jain PK, Singh S, Rizwan-uddin. An exact analytical solution for two-dimensional, unsteady, multilayer heat conduction in spherical coordinates. Int J Heat Mass Transfer 2010;53:2133–42.

[32] Ozisik MN. Heat conduction. 2nd ed. New York: Wiley; 1993.

[33] Fung YC. Foundation of solid mechanics. Englewood Cliffs: Prentice-Hall; 1965.

[34] Powers JM. On the necessity of positive semi-definite conductivity and onsager reciprocity in modeling heat conduction in anisotropic media. J Heat Transfer Trans Asme 2004;126(5):670–5.

[35] Herakovich CT. Mechanics of fibrous composites. New York: Wiley; 1998.

[36] Halpin JC. Primer on composite materials analysis. Boca Raton: CRC Press; 1992.

[37] Bruggeman DAG. Calculation of various physical constants in heterogeneous substances. I: Dielectric constants and conductivity of composites from isotropic substances (German). Ann Phys 1935;24:636–79.

[38] Maxwell JC. A treatise on electricity and magnetism. Third ed. New York: Dover Publications; 1954.

[39] Hashin Z, Shtrikman S. A variational approach to the theory of the effective magnetic permeability of multiphase materials. J Appl Phys 1962;33:1514–7.

[40] Lewis TB, Nielsen LE. Dynamic mechanical properties of particulate-filled polymers. J Appl Polym Sci 1970;14:1449–71.

[41] Torquato S. Bulk properties of two-phase disordered media. I: Cluster expansion for the effective dielectric constant of dispersions of penetrable spheres. J Chem Phys 1984;81:5079–88.

[42] Hasselman DPH, Donaldson KY, Thomas JR. Effective thermal conductivity of uniaxial composite with cylindrically orthotropic carbon fibers and interfacial thermal barrier. J Compos Mater 1993;27:637–44.

[43] Macedo F, Ferreira JA. Thermal contact resistance evaluation in polymer-based carbon fiber. Rev Sci Instrum 2003;74:828–30.

[44] Chapelle E, Garnier B, Bourouga B. Interfacial thermal resistance measurement between metallic wire and polymer in polymer matrix composites. Int J Therm Sci 2009;48:2221–7.

[45] Andrianov IV, Danishevs'kyy VV, Kalamkarov AL. Asymptotic analysis of effective conductivity of composite materials with large rhombic fibers. Compos Struct 2002;56:229–34.

[46] Lee SE, Yoo JS, Kang JH, Kima CG. Prediction of the thermal conductivities of four-axial non-woven composites. Compos Struct 2009;89:262–9.

[47] Arpaci VS. Conduction heat transfer. Massachusetts: Addison-Wesley; 1996.

[48] Myint-U T, Debnath L. Linear partial differential equations for scientists and engineers. Boston: Birkhauser; 2007.

[49] Bahadur R, Bar-Cohen A. Orthotropic thermal conductivity effect on cylindrical pin fin heat transfer. Int J Heat Mass Transfer 2007;50:1155–62.

[50] Siegel R, Howell JR. Thermal radiation heat transfer. Third ed. Washington: Taylor& Francis; 1992.

[51] Singh S, Jain PK, Rizwan-uddin. Analytical solution of time-dependent multilayer heat conduction problems for nuclear applications. In: Proceedings of the first international nuclear and renewable energy conference (INREC10), Amman, Jordan; 2010. p. 1–6.